

## MATCHING THE DARK MATTER PROFILES OF DSPH GALAXIES WITH THOSE OF SIMULATED SATELLITES: A TWO PARAMETER COMPARISON

MAARTEN A. BREDDELS<sup>1</sup>, CARLOS VERA-CIRO<sup>2</sup> AND AMINA HELMI<sup>1</sup>*Draft version July 28, 2015*

## ABSTRACT

We compare the dark matter halos' structural parameters derived for four Milky Way dwarf spheroidal galaxies to those of subhalos found in cosmological  $N$ -body simulations. We confirm that estimates of the mass at a single fixed radius are fully consistent with the observations. However, when a second structural parameter such as the logarithmic slope of the dark halo density profile measured close to the half-light radius is included in the comparison, we find little to no overlap between the satellites and the subhalos. Typically the right mass subhalos have steeper profiles at these radii than measurements of the dSph suggest. Using energy arguments we explore if it is possible to solve this discrepancy by invoking baryonic effects. Assuming that feedback from supernovae can lead to a reshaping of the halos, we compute the required efficiency and find entirely plausible values for a significant fraction of the subhalos and even as low as 0.1%. This implies that care must be taken not to exaggerate the effect of supernovae feedback as this could make the halos too shallow. These results could be used to calibrate and possibly constrain feedback recipes in hydrodynamical simulations.

*Subject headings:* galaxies: dwarf – galaxies: kinematics and dynamics

## 1. INTRODUCTION

The  $\Lambda$ CDM currently favored paradigm of structure formation has proven to be a successful model to explain the evolution and large scale structure of the Universe. It is on small scales, however, where the concordance cosmology faces most of its challenges. One example is the well-known mismatch in the number of observed satellites around systems like the Milky Way and those found in cosmological  $N$ -body simulations (Klypin et al. 1999; Moore et al. 1999). Although this can be solved by invoking baryonic effects, a new problem has been reported regarding the abundance of massive satellites (the so-called “Too Big to Fail problem”, Boylan-Kolchin et al. 2011). Pure  $N$ -body simulations in  $\Lambda$ CDM also predict self-similar halos that have divergent central densities  $\rho \sim r^{-1}$  (Navarro et al. 1996b, 1997). However, models of the internal kinematics of Milky Way dSph have so far yielded inconclusive results regarding the inner slopes of the halos hosting these galaxies (Battaglia et al. 2008; Walker et al. 2009; Breddels & Helmi 2013; Amorisco et al. 2014).

The fundamental question that these studies have tried to address is whether a cusped dark matter density profile fits the observations better than a cored one. This is however, very difficult to answer with current data. For instance, Breddels et al. (2013) using non-parametric orbit-based dynamical models showed that, although small values of the logarithmic inner slope of the dark matter density profile are preferred in the case of the Sculptor dSph, the inner slope value is strongly degenerate with the scale radius and the uncertainties are large. A more feasible task is to measure the logarithmic slope at a finite radius, e.g. at  $r_{-3}$ , the radius where the loga-

rithmic slope of the *light* profile is  $-3$ . Breddels & Helmi (2013, hereafter BH13) have determined the logarithmic slope robustly (i.e. independently of the assumed profile, be it cored or cusped) at  $r_{-3}$ , for the dSph Fornax (Fnx) and Sculptor (Scl), and placed strong constraints on the values for Sextans (Sxt) and Carina (Car). In addition, BH13 confirmed using Schwarzschild modeling, that the mass at this radius can also be tightly constrained (Strigari et al. 2008; Walker et al. 2009; Wolf et al. 2010).

This result shifts the discussion to a better posed question, namely: Are the logarithmic slope and mass at  $r_{-3}$  inferred for these four dwarfs consistent with those found in simulations? This phrasing has the additional advantage that measuring these two quantities in simulations of dwarf galaxies is less prone to numerical artifacts. In this Letter we focus on answering this question using the Aquarius simulations (Springel et al. 2008). Since these simulations do not include baryons, discrepancies could possibly be attributed to missing physics. For instance, early adiabatic contraction could make the density distribution of the central parts steeper (Blumenthal et al. 1986). On the other hand, feedback by supernovae (SNe) may modify the dark matter profile and lead to a shallower inner slope, especially for low mass galaxies (Navarro et al. 1996a; Mashchenko et al. 2006, 2008; Governato et al. 2012; Pontzen & Governato 2012; Teyssier et al. 2013; Di Cintio et al. 2014a,b). Finally, dynamical friction of large baryonic clumps has also been shown to modify the logarithmic slope in the same sense (El-Zant et al. 2001; Goerdt et al. 2006; Nipoti & Binney 2015).

This Letter is structured as follows. In Section 2 we compare the observational results from BH13 to the subhalos from the Aquarius simulations and highlight the discrepancies. In Section 3 we use analytic arguments to estimate the minimum amount of energy needed to transform the subhalos' profiles to a distribution more consistent with the observational constraints following the arguments laid out by Peñarrubia et al. (2012);

e-mail:breddels@astro.rug.nl

<sup>1</sup> Kapteyn Astronomical Institute, University of Groningen, P.O. Box 800, 9700 AV Groningen, The Netherlands<sup>2</sup> Department of Astronomy, University of Wisconsin, 2535 Sterling Hall, 475 N. Charter Street, Madison, WI 53076, USA

Amorisco et al. (2014); Maxwell et al. (2015), and derive the required SNe feedback efficiencies. Finally in Section 4 we discuss the broader implications of our results.

## 2. COMPARISON OF THE DARK HALOS STRUCTURAL PROPERTIES

The Aquarius simulations are a suite of six (labeled Aq-A to Aq-F) high resolution cosmological dark matter only runs of Milky Way-like halos. Here we use the highest resolution simulations available for all six halos (known as level-2), with a particle mass of  $\sim 1.4 \times 10^4 M_\odot$  and a softening length of 66 pc (for more details see Springel et al. 2008). For a more direct comparison of the different systems, we have scaled all halos such that the Milky Way-like hosts have a common mass of  $M_{\text{halo}} = 8.2 \times 10^{11} M_\odot$  (as in Vera-Ciro et al. 2013). A dark halo potentially hosting a galaxy such as Fnx ( $M_{\text{vir}} \sim 10^{9.5} M_\odot$ ) is resolved with  $\sim 2 \times 10^5$  particles, and we expect our results to be reliable beyond a radius of  $\sim 200$  pc, which for Fnx corresponds to  $\sim 0.2 r_{-3}$ .

As mentioned in the Introduction, BH13 have shown that, besides  $M_{-3}$  (the mass within  $r_{-3}$ , Strigari et al. 2008; Walker et al. 2009; Wolf et al. 2010), also  $\gamma_{-3} = d \log \rho_{\text{dm}} / d \log r|_{r_{-3}}$  can be robustly determined for the dSph using current data (see also Wolf & Bullock 2012).  $\gamma_{-3}$  does not depend strongly on the assumed parametric profile that is used, whether cusped, cored or logarithmically cored<sup>3</sup>. These same two quantities can also be estimated for our simulated halos. For each Aquarius satellite we compute both  $M_{-3}$  and  $\gamma_{-3}$  using the values of  $r_{-3}$  measured for each individual dSph galaxy.  $M_{-3}$  follows trivially from the number of particles found within  $r_{-3}$ . We determine the slope  $\gamma$  numerically using the algorithm described in (Lindner et al. 2015). The values obtained are in good agreement with those derived assuming parametric forms for the density profile (such as truncated Einasto or NFW profiles), which are fitted to the data and from which  $\gamma$  can then be computed. Comparing the non-parametric and parametric estimates we gauge the uncertainty on  $\gamma$  to be  $\sim 0.2$ .

In Fig. 2, we show the posteriors for the joint distribution of  $M_{-3}$  and  $\gamma_{-3}$  derived by BH13 separately for each dSph galaxy. The red contours correspond to the 1 and 2  $\sigma$  equivalent contours for the NFW (Navarro et al. 1996b, 1997) profile

$$\rho_{\text{dm}}(r) = \rho_0 \frac{1}{r/r_s (1 + r/r_s)^2}, \quad (1)$$

while green corresponds to the logarithmic cored profile (core13 in the nomenclature of BH13)

$$\rho'_{\text{dm}}(r) = \rho'_0 \frac{1}{(1 + r/r'_s)^3}, \quad (2)$$

where  $r_s$  and  $r'_s$  are the scale radii and  $\rho_0$  and  $\rho'_0$  characteristic densities. We also plot in these panels the subhalos' structural parameters determined non-parametrically and computed at the  $r_{-3}$  of the corresponding dSph. We show here only those subhalos that host a luminous galaxy according to the semi-analytic

<sup>3</sup> A distinction is made between strictly cored ( $\lim_{r \rightarrow 0} d \rho_{\text{dm}} / dr = 0$ ), and logarithmically cored ( $\lim_{r \rightarrow 0} d \log \rho_{\text{dm}} / d \log r = 0$ ).

model of Starkenburg et al. (2013). The black dots correspond to all such subhalos present in the six scaled Aquarius simulations, while the colored triangles are those that host a galaxy with an absolute magnitude within  $\pm 0.75$  of the respective dSph.

From the top left panel, we see that the subhalos overlap little with Fnx, especially if only the correct luminosity range is considered. Note that if one only compares the  $M_{-3}$  values, then some subhalos with the right luminosity do actually match. Also if only the slope  $\gamma_{-3}$  were to be taken into account, several subhalos would be compatible with the observational constraints.

However the discrepancy becomes noteworthy for Fnx when comparing the observations and simulations in the two-dimensional space spanned by  $M_{-3}$  and  $\gamma_{-3}$ . For Scl and Car there is some, although small, amount of overlap with the subhalos, but this is less so for Sxt. Both Car and Sxt have large uncertainties on the slope estimate, which makes the comparison less conclusive.

Therefore it is clear that these four dwarfs all show a systematic deviation from the simulations: the slope of their dark matter profiles are shallower than those found in the Aquarius simulations, even if subhalos with a broader range of luminosities are considered.

## 3. RESHAPING DARK MATTER HALOS

As we have just seen dark matter only simulations in the  $\Lambda$ CDM cosmology, predict steeper slopes of the dark matter profiles than those determined for the dSphs. The most commonly proposed mechanism to transform the shape of the dark matter profile is feedback from SNe that affects the baryons and, through gravity, ultimately alters the dark matter mass distribution in these systems (Mashchenko et al. 2006, 2008; Governato et al. 2012; Pontzen & Governato 2012; Teyssier et al. 2013; Di Cintio et al. 2014b).

To establish whether a given Aquarius subhalo can be reshaped into a halo that is compatible with a dSph, we first need to know how much energy is required to do the transformation. Following Peñarrubia et al. (2012) we assume that each dwarf is in virial equilibrium, and we compute the energy needed to transform a subhalo  $i$  to match the dSph model  $j$  (given by Eq. (1) and Eq. (2)):  $\delta E = (W_{\text{dSph}} - W_{\text{sub}}) / 2$ . Here  $W_{\text{sub}}$  is the potential energy of the subhalo and  $W_{\text{dSph}}$  is the potential energy of the best fitting model for our dSph:

$$W_{\text{dSph}} = -4\pi G \int_0^{r_{\text{max},i}} dr \rho_{\text{dm},j}(r) M_j(r) r, \quad (3)$$

with  $M(r) = M_{\text{dm}}(r)$ , i.e. we ignore the baryonic component which is sub-dominant for dSph. We choose two different values of  $r_{\text{max}}$ , namely  $r_{50}$  and  $r_{95}$ , the radii enclosing 50% or 95% of the bound mass of each subhalo. The potential energy at  $r_{95}$  is more negative than at  $r_{50}$ , and thus the energy required to transform the system inside  $r_{50}$  is smaller than that required for  $r_{95}$ . (Note that these values are larger than those used by Maxwell et al. (2015), who took  $r_{\text{max}} = 3r_c$ , with  $r_c$  the radius where the dark halo profile's logarithmic slope is  $-0.5$ ).

We calculate  $W_{\text{sub}}$  directly using the particles from the

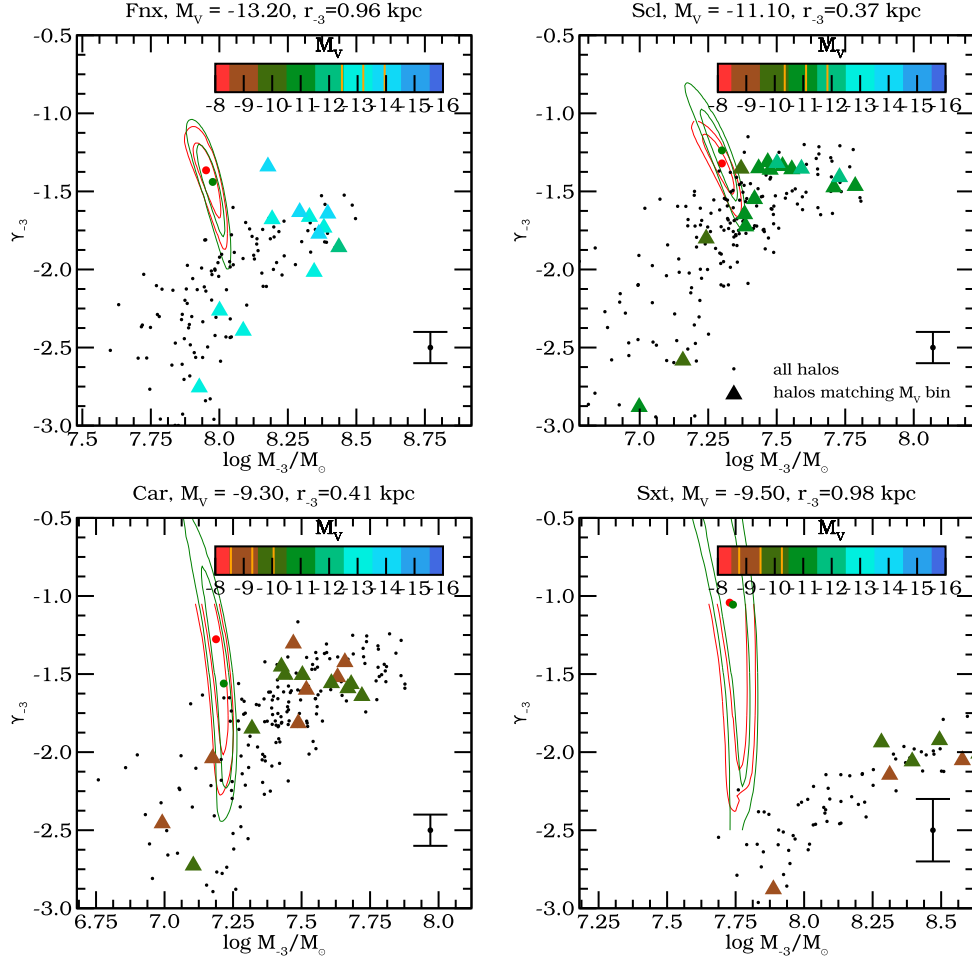


FIG. 1.— Joint probability distribution function for the logarithmic slope  $\gamma_{-3}$  and mass  $M_{-3}$  of the dark matter halo at  $r_{-3}$  for our sample of dSph. The contours represent the  $1\sigma$  and  $2\sigma$ -equivalent confidence regions for an NFW profile (red, Eq. (1)) and the **core13** model (green, Eq. (2)). The black points correspond to the subhalos of the six scaled Aquarius Milky Way-like halos, while the colored triangles are the subset with luminosity within  $\pm 0.75$  of the value of the respective dSph as predicted by the semi-analytic model of [Starkenburg et al. \(2013\)](#). The error bar on the bottom right indicates the uncertainty in the slope estimated for the simulations.

dark matter simulations:

$$\begin{aligned}
 W_{\text{sub}} &= -4\pi G \int_0^{r_{\text{max},i}} dr \rho_{\text{dm},i}(r) M_i(r) r \\
 &= -G \int_0^{r_{\text{max},i}} dM M_i(r)/r \\
 &= -G \sum_{k=1}^N m^2 k/r_k,
 \end{aligned} \tag{4}$$

where  $m$  is the dark matter particle mass,  $r_k$  is the sorted radial distance of particle  $k$  from the center of the subhalo such that  $r_1$  is the innermost particle and  $r_N$  that farthest away but still within  $r_{\text{max}}$ .

Fig. 2 shows for each dSph the ratio  $W_{\text{dSph}}/W_{\text{sub}}$  as a function of absolute magnitude  $M_V$  as given by the semi-analytic model. The blue bands indicate a magnitude range of  $\pm 0.75$  around the corresponding dSph. The solid circles are for the NFW (red) and **core13** (green) best fit models computed for  $r_{95}$  while the triangles are for  $r_{50}$ .

When the ratio  $W_{\text{dSph}}/W_{\text{sub}} < 1$  (all symbols *below* the black horizontal line) objects need energy to transform their halos. In these cases the binding energy of the

resulting object is larger (less negative) than that of the original untransformed subhalo. When  $W_{\text{dSph}}/W_{\text{sub}} > 1$  (all symbols *above* the black horizontal line) the binding energy of the resulting object is smaller and such objects would have to lose energy to be transformed into a profile that matches the observations. Regardless of the mechanism, this transformation is energetically possible and we do not discuss it further.

As in [Peñarrubia et al. \(2012\)](#), we estimate the total available energy from SNe as

$$E_{\text{SN,total}} = \frac{M_{\star}}{\langle m_{\star} \rangle} \xi(m_{\star} > 8M_{\odot}) E_{\text{SN}}, \tag{5}$$

where  $\xi(m_{\star} > 8M_{\odot}) = 0.0037$  and  $\langle m_{\star} \rangle = 0.4M_{\odot}$ . If the energy needed to transform a given halo is larger than what can be delivered from SNe (i.e. the SN efficiency is larger than 100%), we plot it in Fig. 2 with an open symbol. Note that for Fornax only a few open symbols exist. This means that almost all of the candidate subhalos could be reshaped into Fornax given its stellar content and the energy available from SNe.

For each dSph, we plot in Fig. 3 the ratio of the energy required to transform the system to the SN energy

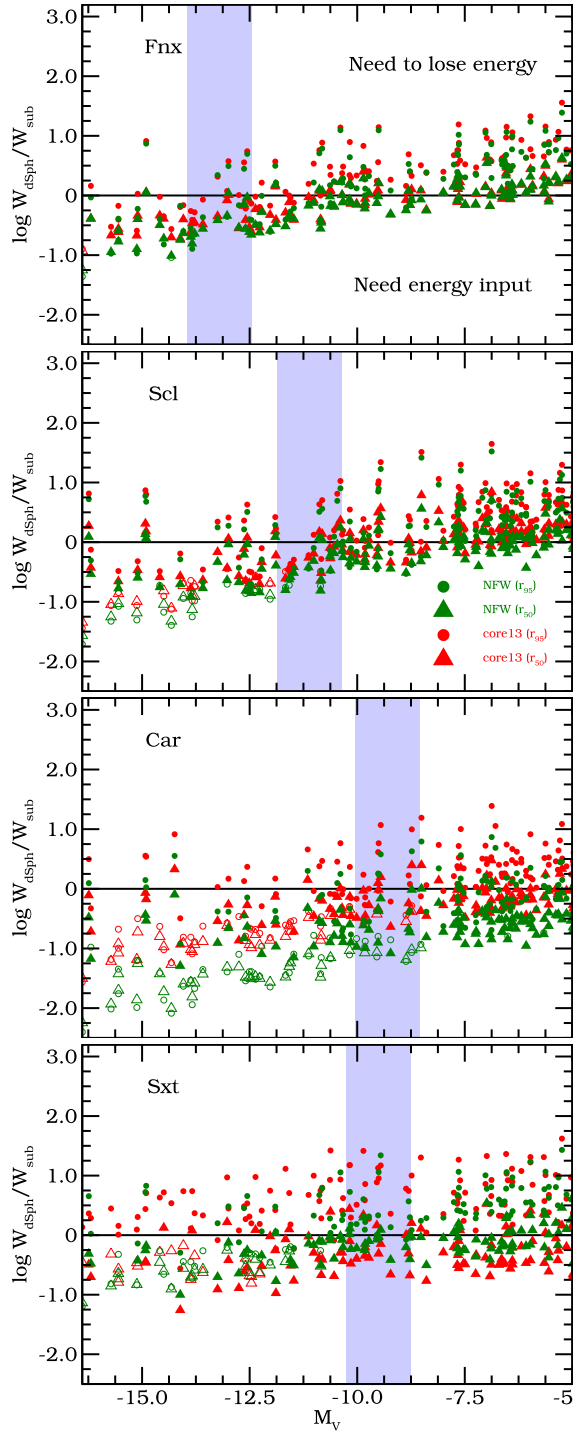


FIG. 2.— Ratio of the potential energy of the dSph,  $W_{\text{dsph}}$ , to that of the Aquarius subhalos  $W_{\text{sub}}$ , as a function of their predicted absolute magnitude  $M_V$ , computed for  $r_{95}$  (circles) and  $r_{50}$  (triangles) for the NFW (red) and **core13** (green) models. The blue band indicates an absolute magnitude range within  $\pm 0.75$  of the of the corresponding dSph. The open symbols are subhalos which cannot be transformed with the energy available in SNe.

output as estimated above, i.e.  $\varepsilon_{\text{SN}} = \delta E / E_{\text{SN, total}}$  is the SN efficiency needed to do the transformation. We thus only plot the objects which lie below the horizontal lines in Fig. 2. This analysis reveals that for each dSph, subhalos with the right luminosities exist which can be

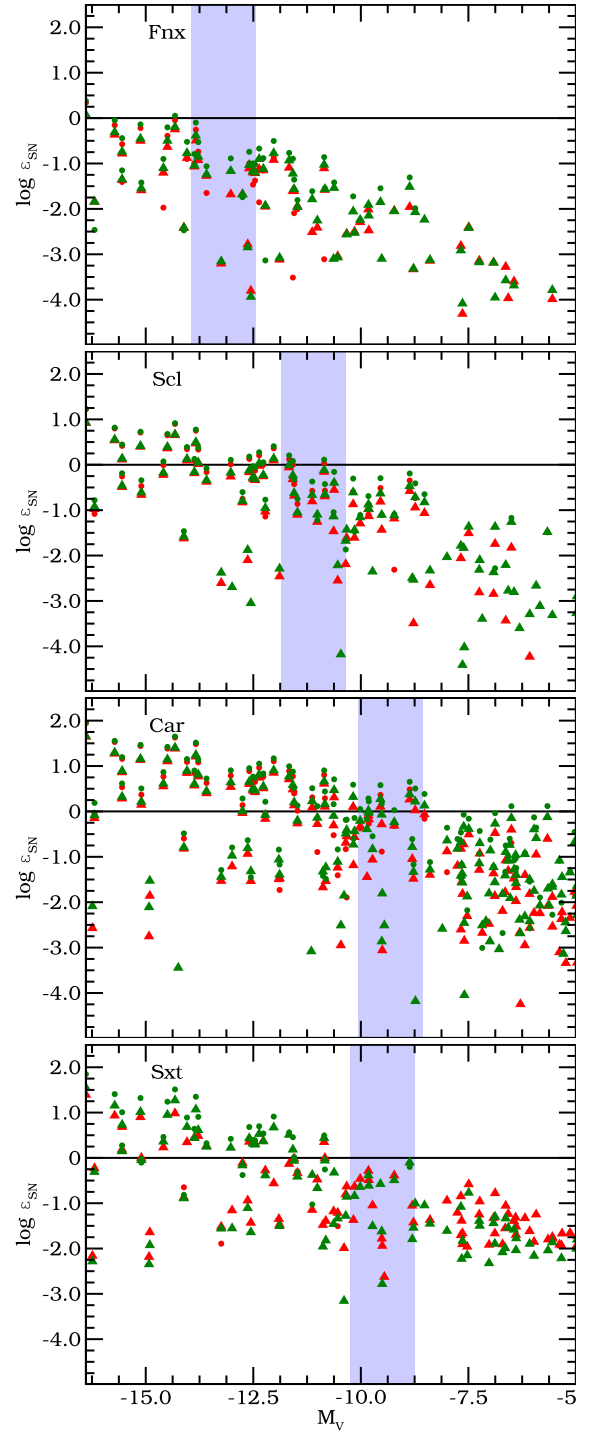


FIG. 3.— Similar to Fig 2, now showing the SN efficiency needed to transform the Aquarius halos.

reshaped to follow a dark matter profile consistent with the observations. The required efficiencies range from  $\sim 0.1\%$  up to slightly more than 100%, depending somewhat on the extent of the region of the subhalo that would be transformed ( $r_{50}$  or  $r_{95}$ ). Furthermore there is always at least one subhalo that requires a SN feedback efficiency  $\varepsilon_{\text{SN}} < 0.001$ .

#### 4. DISCUSSION AND CONCLUSIONS



We have shown that in the two dimensional parameter space defined by the mass and the logarithmic slope of the dark matter density profile at  $r_{-3}$ , the Milky Way’s dSph do not match the predictions from dark matter only simulations. While in [Vera-Ciro et al. \(2013\)](#) we argued that by rescaling the Milky Way mass to a (low) value of  $\sim 8 \times 10^{11} M_{\odot}$  we could circumvent the so called “Too Big Too Fail Problem”, we now see that halos with the right mass, do not have the right logarithmic slope at  $r_{-3}$ . However, baryons can have a considerable effect on the shape of the dark matter density profile through feedback (e.g. [Governato et al. 2012](#)). We have shown here that it is energetically possible at redshift of  $z = 0$  to reshape the simulated halos and make them compatible with the observations. Note that this process would require even less energy at higher redshift, as discussed by [Amorisco et al. \(2014\)](#); [Madau et al. \(2014\)](#).

Hydrodynamical (cosmological) simulations of (isolated) dwarf galaxies are now available in the literature (e.g. [Teyssier et al. 2013](#); [Di Cintio et al. 2014a,b](#); [Sawala et al. 2015](#)), and are more representative of galaxy formation scenarios in  $\Lambda$ CDM, since they self consistently include baryonic physics. [Di Cintio et al. \(2014b\)](#), for instance, predicts the slope in a given radial range to be predominantly dependent of the ratio  $M_{\star}/M_{\text{halo}}$ . In their simulations an object like Fnx (whose  $M_{\star} = 4 \times 10^7 M_{\odot}$ , [de Boer et al. 2012](#)), is embedded in dark matter halo of virial mass  $M_{\text{halo}} \sim 10^{10} - 10^{10.5} M_{\odot}$ . Such objects are reported to have dark halo profile’s logarithmic slopes  $\alpha \in [-1, -0.5]$  for the radial range  $0.8 - 1.8$  kpc. This is inconsistent at a  $2\sigma$  level with our measurement of the slope for Fnx at  $r_{-3} \sim 1$  kpc as can be seen from [Fig. 2](#). Such simulations therefore, predict slopes that are too shallow compared to the observationally determined val-

ues (see also [Madau et al. 2014](#); [Chan et al. 2015](#)). This suggests that the feedback scheme used might be too strong for objects of this mass scale.

It is more difficult to make a detailed and conclusive comparison the other dSph because the simulations’ suites available in the literature do not contain such faint objects or the ranges in which the slopes are measured are typically larger than the observed  $r_{-3}$ .

The steep slopes (corresponding to high concentration) of low mass dark halos could be another manifestation of the “Too Big to Fail” problem (however see [Papastergis et al. 2015](#)), although the two issues are not necessarily strictly related, since other solutions to this problem exist ([Wang et al. 2012](#); [Vera-Ciro et al. 2013](#); [Brooks & Zolotov 2014](#); [Arraki et al. 2014](#)). For example, [Brooks & Zolotov \(2014\)](#) argue that efficient feedback solves it, but the preliminary comparisons made above show that a careful treatment is required. We hope that our measurements of the logarithmic slopes and masses of dSph can be used to better constrain poorly understood processes such as the interplay between adiabatic contraction and supernova feedback in these small mass systems.

AH and MB are grateful to NOVA for financial support. AH acknowledges financial support the European Research Council under ERC-Starting Grant GALACTICA-240271. The Aquarius simulations have been run by the VIRGO consortium, and we are very grateful to this collaboration, and particularly indebted to Volker Springel. We are especially thankful to Else Starkenburg for the outputs of the semi-analytic code used in this Letter, and also to Gabriella De Lucia and Yang-Shyang Li for the contributions to its development.

## REFERENCES

- Amorisco, N. C., Zavala, J., & de Boer, T. J. L. 2014, *ApJ*, 782, L39 [1, 4](#)
- Arraki, K. S., Klypin, A., More, S., & Trujillo-Gomez, S. 2014, *MNRAS*, 438, 1466 [4](#)
- Battaglia, G., Helmi, A., Tolstoy, E., et al. 2008, *ApJ*, 681, L13 [1](#)
- Blumenthal, G. R., Faber, S. M., Flores, R., & Primack, J. R. 1986, *ApJ*, 301, 27 [1](#)
- Boylan-Kolchin, M., Bullock, J. S., & Kaplinghat, M. 2011, *MNRAS*, 415, L40 [1](#)
- Breddels, M. A., & Helmi, A. 2013, *A&A*, 558, A35 [1](#)
- Breddels, M. A., Helmi, A., van den Bosch, R. C. E., van de Ven, G., & Battaglia, G. 2013, *MNRAS*, 433, 3173 [1](#)
- Brooks, A. M., & Zolotov, A. 2014, *ApJ*, 786, 87 [4](#)
- Chan, T. K., Kereš, D., Oñorbe, J., et al. 2015, *ArXiv e-prints*, arXiv:1507.02282 [4](#)
- de Boer, T. J. L., Tolstoy, E., Hill, V., et al. 2012, *A&A*, 544, A73 [4](#)
- Di Cintio, A., Brook, C. B., Dutton, A. A., et al. 2014a, *MNRAS*, 441, 2986 [1, 4](#)
- Di Cintio, A., Brook, C. B., Macciò, A. V., et al. 2014b, *MNRAS*, 437, 415 [1, 3, 4](#)
- El-Zant, A., Shlosman, I., & Hoffman, Y. 2001, *ApJ*, 560, 636 [1](#)
- Goerdt, T., Moore, B., Read, J. I., Stadel, J., & Zemp, M. 2006, *MNRAS*, 368, 1073 [1](#)
- Governato, F., Zolotov, A., Pontzen, A., et al. 2012, *MNRAS*, 422, 1231 [1, 3, 4](#)
- Klypin, A., Kravtsov, A. V., Valenzuela, O., & Prada, F. 1999, *ApJ*, 522, 82 [1](#)
- Lindner, R. R., Vera-Ciro, C., Murray, C. E., et al. 2015, *AJ*, 149, 138 [2](#)
- Madau, P., Shen, S., & Governato, F. 2014, *ApJ*, 789, L17 [4](#)
- Mashchenko, S., Couchman, H. M. P., & Wadsley, J. 2006, *Nature*, 442, 539 [1, 3](#)
- Mashchenko, S., Wadsley, J., & Couchman, H. M. P. 2008, *Science*, 319, 174 [1, 3](#)
- Maxwell, A. J., Wadsley, J., & Couchman, H. M. P. 2015, *ApJ*, 806, 229 [1, 3](#)
- Moore, B., Ghigna, S., Governato, F., et al. 1999, *ApJ*, 524, L19 [1](#)
- Navarro, J. F., Eke, V. R., & Frenk, C. S. 1996a, *MNRAS*, 283, L72 [1](#)
- Navarro, J. F., Frenk, C. S., & White, S. D. M. 1996b, *ApJ*, 462, 563 [1, 2](#)
- . 1997, *ApJ*, 490, 493 [1, 2](#)
- Nipoti, C., & Binney, J. 2015, *MNRAS*, 446, 1820 [1](#)
- Papastergis, E., Giovanelli, R., Haynes, M. P., & Shankar, F. 2015, *A&A*, 574, A113 [4](#)
- Peñarrubia, J., Pontzen, A., Walker, M. G., & Koposov, S. E. 2012, *ApJ*, 759, L42 [1, 3, 3](#)
- Pontzen, A., & Governato, F. 2012, *MNRAS*, 421, 3464 [1, 3](#)
- Sawala, T., Frenk, C. S., Fattahi, A., et al. 2015, *MNRAS*, 448, 2941 [4](#)
- Springel, V., Wang, J., Vogelsberger, M., et al. 2008, *MNRAS*, 391, 1685 [1, 2](#)
- Starkenburg, E., Helmi, A., De Lucia, G., et al. 2013, *MNRAS*, 429, 725 [2, 1](#)
- Strigari, L. E., Bullock, J. S., Kaplinghat, M., et al. 2008, *Nature*, 454, 1096 [1, 2](#)
- Teyssier, R., Pontzen, A., Dubois, Y., & Read, J. I. 2013, *MNRAS*, 429, 3068 [1, 3, 4](#)
- Vera-Ciro, C. A., Helmi, A., Starkenburg, E., & Breddels, M. A. 2013, *MNRAS*, 428, 1696 [2, 4](#)
- Walker, M. G., Mateo, M., Olszewski, E. W., et al. 2009, *ApJ*, 704, 1274 [1, 2](#)
- Wang, J., Frenk, C. S., Navarro, J. F., Gao, L., & Sawala, T. 2012, *MNRAS*, 424, 2715 [4](#)

Wolf, J., & Bullock, J. S. 2012, ArXiv e-prints, arXiv:1203.4240 [2](#)

Wolf, J., Martinez, G. D., Bullock, J. S., et al. 2010, MNRAS, 406, 1220 [1](#), [2](#)